J. Membrane Biol. 145, 233–244 (1995)

The Journal of
Membrane
Biology

Modulation of Neuronal Calcium Channels by Arachidonic Acid and Related Substances

H. Schmitt*, H. Meves

I. Physiologisches Institut der Universität des Saarlandes, D-66421 Homburg/Saar, Federal Republic of Germany

Received: 4 November 1994/Revised: 15 February 1995

Abstract. Low-voltage-activated (l-v-a) and high-voltage-activated (h-v-a) Ca^{2+} currents (I_{Ca}) were recorded in whole-cell voltage clamped NG108-15 neuroblastoma x glioma hybrid cells. We studied the effects of arachidonic acid (AA), oleic acid, myristic acid and of the positively charged compounds tetradecyltrimethylammonium (C_{14}TMA) and sphingosine. At pulse potentials >–20 mV, AA (25–100 μM) decreased l-v-a and h-v-a I_{Ca} equally. The decrease developed slowly and became continually stronger with increasing time of application. It was accompanied by a small negative shift and a slight flattening of the activation and inactivation curves of the l-v-a I_{Ca}. The shift of the activation curve manifested itself in a small increase of l-v-a I_{Ca} at pulse potentials <–30 mV. The effects were only partly reversible. The AA effect was not prevented by 50 μM 5, 8, 11, 14-eicosatetraynoic acid, an inhibitor of the AA metabolism, and not mimicked by 0.1–1 μM phorbol 12, 13-dibutyrate, an activator of protein kinase C. Probably, AA directly affects the channel protein or its lipid environment. Oleic and myristic acid acted similarly to AA but were much less effective. The positively charged compounds C_{14}TMA and sphingosine had a different effect: They shifted the activation curve of l-v-a I_{Ca} in the positive direction and suppressed l-v-a more than h-v-a I_{Ca}; their effect reached a steady-state within 5–10 min and was readily reversible. C_{14}TMA blocked l-v-a I_{Ca} with an IC_{50} of 4.2 μM while sphingosine was less potent.

Key words: Ca^{2+} current — Arachidonic acid — Myristic acid — Tetradecyltrimethylammonium — Sphingosine — Neuroblastoma x glioma hybrid cells

* *Present Address:* Max-Planck-Institut für Medizinische Forschung, D-69120 Heidelberg

Correspondence to: H. Meves

Introduction

Arachidonic acid (AA) modulates ionic channels, either activating or inhibiting them. In many cases, the fatty acid directly affects the channel protein or its lipid environment, in other cases it acts through one of its metabolites, in still others via activation of protein kinase C (PKC) (for review of the literature, *see* [21]).

The starting point for our experiments was the recent work of Ordway et al. and Petrou et al. [23–26]. They found that AA directly activates K^+ channels in smooth muscle cells of the toad stomach [23, 24]. The effect is shared by other negatively charged lipids (e.g., myristic acid, oleic acid or lysophosphatidate) whereas positively charged lipids (e.g., sphingosine) suppress activity and neutral compounds (e.g., alcohols) have no effect [25]. In the NMDA receptor, whose current is also potentiated by AA [22], a 131-residue domain can be identified that resembles known fatty-acid binding proteins, supporting — for this particular channel — the idea of a direct interaction between AA and channel protein [26].

We studied the effect of AA on the Ca^{2+} currents of NG108-15 mouse neuroblastoma x rat glioma hybrid cells, a cell line that has proved useful for recording both low-voltage-activated (l-v-a) and high-voltage-activated (h-v-a) Ca^{2+} currents [3, 33]. As briefly mentioned in a previous publication [29], 25 μM AA partly blocks the l-v-a I_{Ca} of NG108-15 cells. The literature reports inhibitory effects on h-v-a I_{Ca} in other cells, e.g., in hippocampal neurons [17] and intestinal smooth muscle [32]. We started by asking three questions: (i) Does AA block l-v-a and h-v-a I_{Ca} to the same extent? (ii) Is it a direct AA effect as described by [23–26] and can it be mimicked by other fatty acids or lysophosphatidate? (iii) Do positively charged compounds with long hydrophobic tails such as tetradecyltrimethylammonium (C_{14}TMA) or sphingosine act differently?

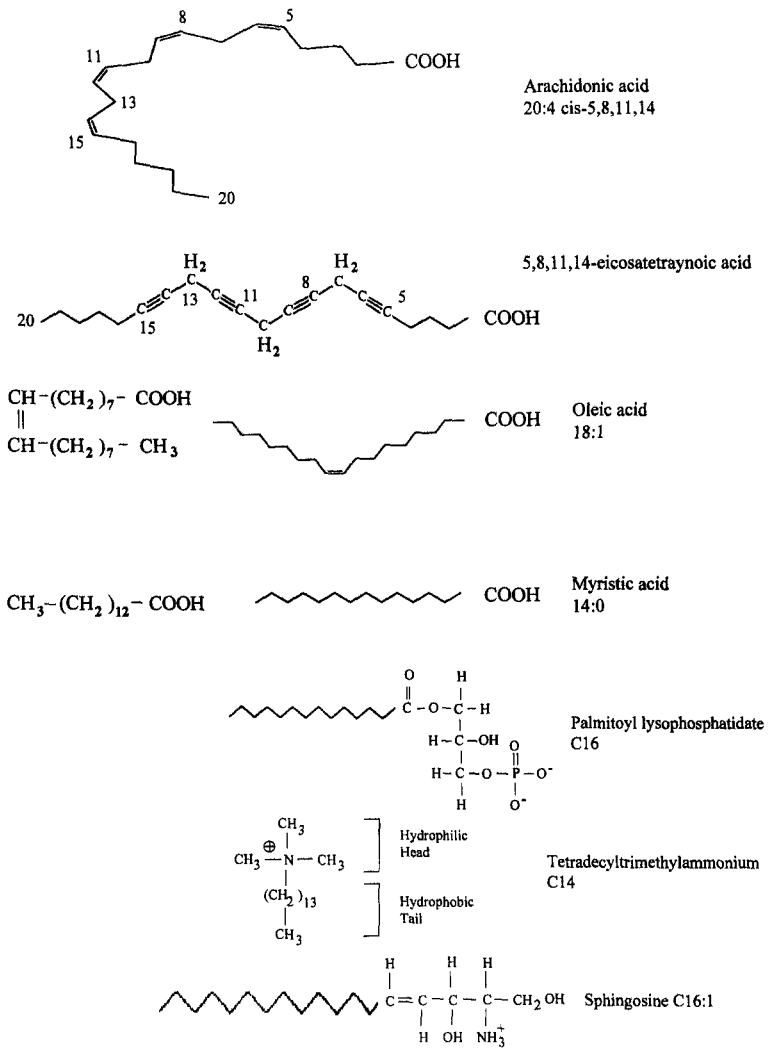

Fig. 1. Structural formulae of the substances used.

The structural formulae of the substances that we studied are shown in Fig. 1. Some of our results have been reported in abstract form [30].

Materials and Methods

Mouse neuroblastoma x rat glioma hybrid cells, clone NG108-15, of passage numbers between 14 and 50 were grown in Dulbecco's modified Eagle's medium (DMEM) supplemented with 10% fetal calf serum and hypoxanthine, aminopterin and thymidine. For the experiments, the cells were plated at a density of about 5×10^4 cells/35-mm-diameter culture dish and induced to differentiate by DMEM containing 1% fetal calf serum, hypoxanthine and thymidine, 10 μM prostaglandin E_1 and either 1 mM theophylline or 50 μM isobutylmethylxanthine for 6–10 days prior to recording.

Cells were voltage-clamped in the whole-cell mode, using an EPC-7 amplifier (List Electronics) and pipettes with 2–4 MΩ resistance, and continuously superfused by the bath solution (flow rate 1–2 ml/min). The holding potential was –80 mV in early experiments and –70 mV in the later experiments including those of Figs. 2–7. The volume of the recording chamber was reduced to about 1 ml by inserting a perspex ring (internal and external diameter 15 and 35 mm, respectively) into the culture dish. The cell diameter was 20–60 μm and the cell capacitance (read from the C-slow setting of the EPC-7) 30–100 pF. The experiments were done at room temperature (20–22°C).

The composition of the bath and pipette solutions is given in the Table. The cesium (Cs) and tetraethylammonium (TEA) in the bath and pipette solution served to block potassium currents. Sodium currents were blocked by 0.2 μM tetrodotoxin (TTX) in the bath. In the early experiments, external Ba^{2+} was used as a charge carrier to enhance current through Ca^{2+} channels. Run down of the Ca^{2+} currents was found minimal in the bath solution with 10 mM $CaCl_2$ and the pipette solution with 100 mM Cs methylsulfonate (osmolarity 305 and 284 mOsm, respectively). These became the preferred solutions and were used for the experiments shown in Figs. 2–7. In experiments with palmitoyl lysophosphatidate (PLP), $MgCl_2$ was omitted from the bath solution to avoid complex formation (*see* [25]).

Arachidonic acid (AA) and the other test substances (except PLP) were dissolved in dimethylformamide (DMF) in concentrations between 10 and 100 mM. PLP (116 mM) came dissolved in chloroform. Appropriate amounts of these stock solutions were added to 50 ml bath solution immediately before use. Bath solutions with AA or PLP were bubbled with N_2, sonicated for 7 min and kept in the dark. Bath solutions with oleic or myristic acid were also sonicated. The final DMF or chloroform concentration never exceeded 0.1%.

Cs methylsulfonate was bought from Aldrich, TEA from Fluka, TTX from Sankyo, PLP from Avanti Polar Lipids, AA from Larodan

Table. Composition of solutions

Bath solutions										
$CaCl_2$ or $BaCl_2$ (mM)	NaCl (mM)	KCl (mM)	TEACl (mM)	CsCl (mM)	$MgCl_2$ (mM)	glucose (mM)	TTX (μM)	Hepes (mM)	pH	
10 $CaCl_2$	100	0	35	5	1	5	0.3	5	7.4	
10 $BaCl_2$	100	0	25	5	0	10	0.1	10	7.4	
50 $BaCl_2$	30	0	25	5	0	25	0.1	10	7.4	
Pipette solutions										
Main internal salt (mM)	NaCl (mM)	KCl (mM)	CsCl (mM)	$MgCl_2$ (mM)	EGTA (mM)	$CaCl_2$ (mM)	glucose (mM)	Na_2ATP (mM)	Hepes (mM)	pH
130 Cs glutamate	16	0	0	2.5	10	0.1	5	0	20	7.15
100 Cs methylsulfonate	0	0	30	0	5	0.5	0	0	10	7.20

AB (Sweden) or Sigma and all other substances from Sigma. We used the bromide salt of $C_{14}TMA$.

Membrane currents were corrected for capacitative and leakage currents; for this purpose the current produced by a 30 mV hyperpolarizing pulse was added after appropriate scaling.

To obtain the inactivation curve of the l-v-a Ca^{2+} current, 800 msec prepulses of varying size were used, followed after a 10 msec pause by a 200 msec test pulse to −10 mV (Fig. 5) or −20 mV. The difference between peak test pulse current and current at the end of the test pulse was plotted against prepulse potential. The points were fitted by the equation

$$I = I_{max}/\{1 + \exp[(V\text{-}V_o)/k]\} \quad (1)$$

where I_{max} is the maximum current, V_o the potential at which I equals half I_{max} and k a reciprocal measure of the slope in terms of millivolts per e-fold change.

Eq. (1) with negative k values was used to fit the activation curve of the l-v-a Ca^{2+} channels. The latter was obtained by plotting l-v-a Ca^{2+} current (I) divided by its maximum (I_{max}) against pulse potential V (*see* [1]).

For the concentration-response curve in Fig. 3 we used the equation

$$I_{AA}/I_{control} = 1/\{1+([AA]/IC_{50})^n\} \quad (2)$$

with I_{AA} and $I_{control}$ denoting the current in *AA* and control, respectively, [*AA*] the *AA* concentration, IC_{50} the *AA* concentration producing 50% inhibition and n the Hill coefficient. A corresponding equation for $C_{14}TMA$ was used in Fig. 7.

Wherever possible, averages ±SEM are given. We used the two-tailed, unpaired *t*-test to decide whether the difference between two average values is significant at the 5% level.

Results

General Observations

Differentiated NG108-15 cells generally have low-voltage-activated (l-v-a), fast inactivating as well as high-voltage-activated (h-v-a), slowly inactivating Ca^{2+} currents whose activation is first seen at −40 and 0 mV, respectively [3, 33]. We often saw a conspicuous kink in the current-voltage curve at 0 or 10 mV, especially with 10 mM $CaCl_2$ as bath and 100 mM methylsulfonate in the pipette (Fig. 2*A*). Prepulse experiments, which are described later (Fig. 4), support the view that I_{Ca} at $V < 0$ mV is almost exclusively l-v-a I_{Ca} whereas at $V > +20$ mV h-v-a I_{Ca} prevails.

In most experiments the l-v-a Ca^{2+} current increased slowly with time whereas the h-v-a Ca^{2+} current decreased continually. The increase of the former was probably caused by a slow shift of the activation curve to more negative values of membrane potential. Such a negative shift has been reported before, e.g., [5, 9]. In the first 10 min after break-through to whole-cell mode the increase of the l-v-a Ca^{2+} current measured at −40 mV was 14.5%/min in Fig. 2 (*see* broken line). In agreement with [9], the increase was much smaller at later times. The decrease of the h-v-a Ca^{2+} current was most pronounced with 50 mM $BaCl_2$ and 130 mM Cs glutamate (for similar observations on NIE-115 neuroblastoma cells, *see* [12]) and often totally absent with 10 mM $CaCl_2$ as bath and 100 mM Cs methylsulfonate in the pipette.

25 μM AA Decreases L-v-a and H-v-a Ca^{2+} Current

A 15-min application of 25 μM AA reduced I_{Ca} at all potentials between −30 and +80 mV and increased it at −50 and −40 mV (Fig. 2*A*). As shown by the inset, the reduction in current amplitude was not accompanied by a change in kinetics. The effect of AA developed slowly and became continually stronger with increasing time of application. This is illustrated by Fig. 2*B* which shows the peak I_{Ca} at three different potentials (−40, −20 and +30 mV) plotted against time. While the currents at −20 and +30 mV decreased slowly, the current at −40 mV increased slightly. The dotted line fitted to the three control points at −40 mV and extrapolated to 25 min shows that part of this increase occurred spontaneously, i.e., was not caused by AA.

For a quantitative analysis, we measured the peak Ca^{2+} currents at −20 or −10 mV and at +20 mV, i.e., l-v-a and h-v-a I_{Ca}, respectively. On average, lumping the experiments with different bath and pipette solutions (*see* Materials and Methods), a 10-min application of 25 μM AA reduced l-v-a I_{Ca} to 84.1 ± 3.8% of control (n = 17)

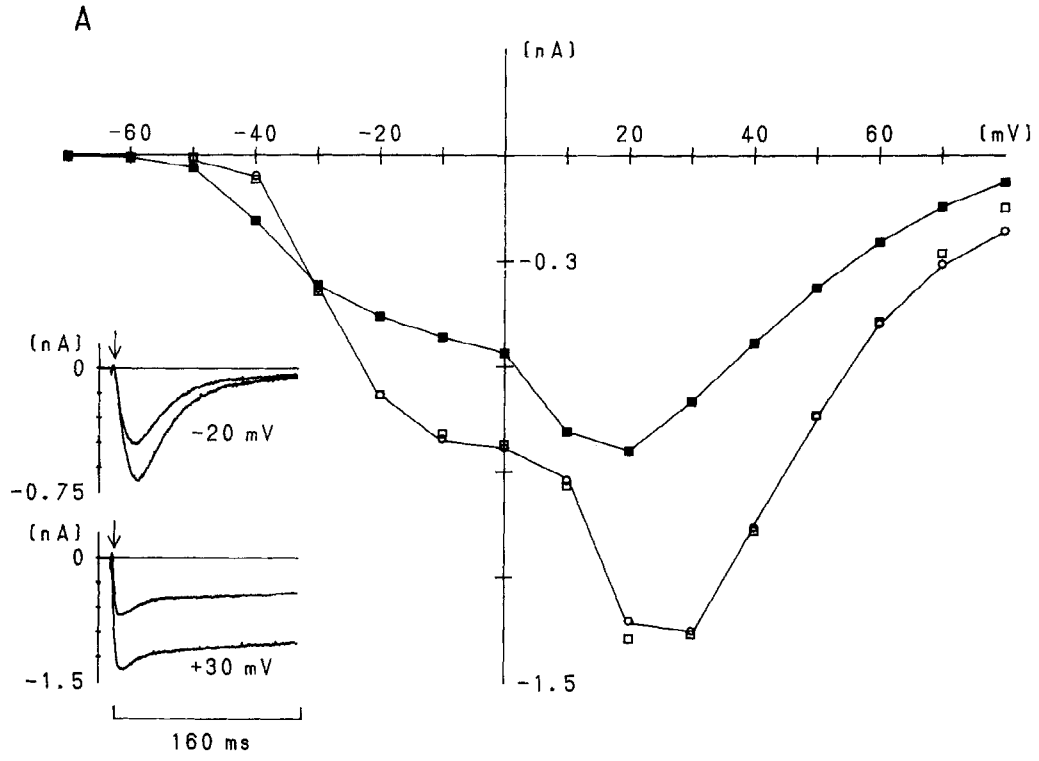

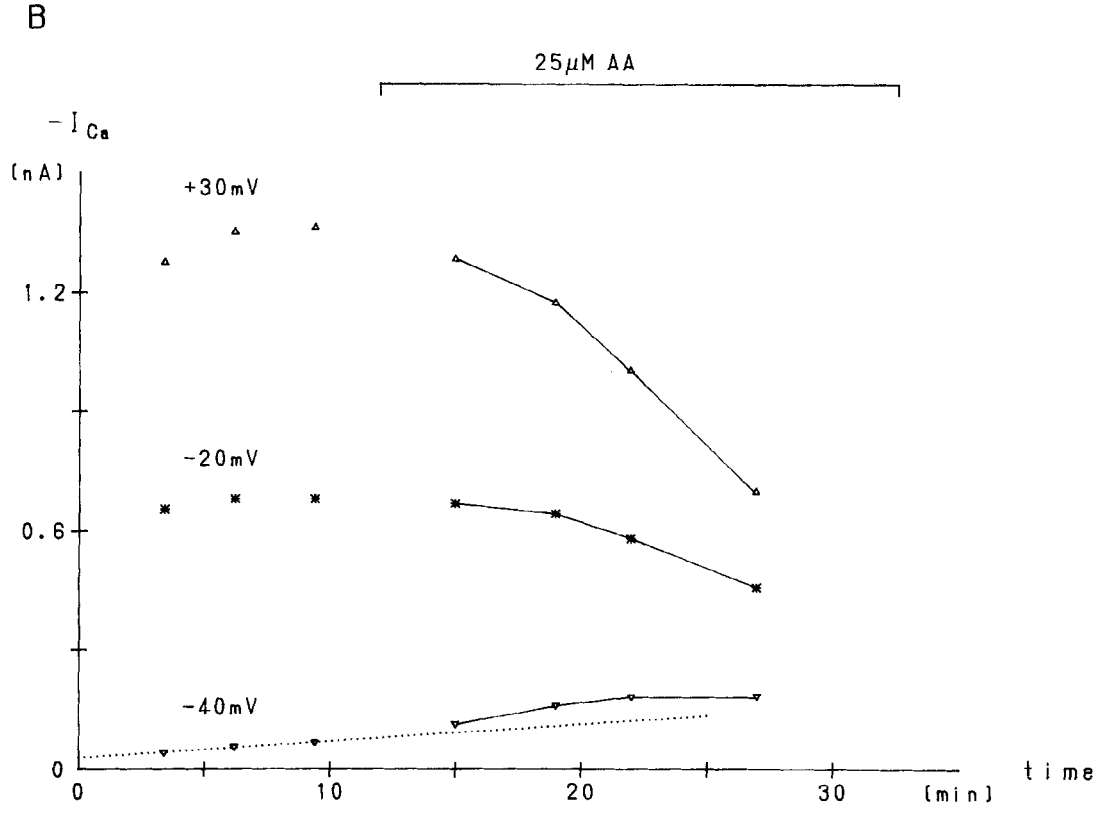

Fig. 2. Effect of 25 μM AA on the l-v-a and h-v-a Ca^{2+} current. (*A*) Current-voltage curve. ○ and □, first and second control (3 min apart); ■, 25 μM AA applied for 15 min. Inset: Currents in control and 25 μM AA (smaller currents) at −20 and +30 mV (pulse begin marked by arrow). (*B*) Peak currents at −40, −20 and +30 mV *vs.* time after break-through to whole-cell mode. Broken straight line fitted to first three points (control) at −40 mV to indicate slow spontaneous increase of I_{Ca} at −40 mV. Cell capacitance 60 pF.

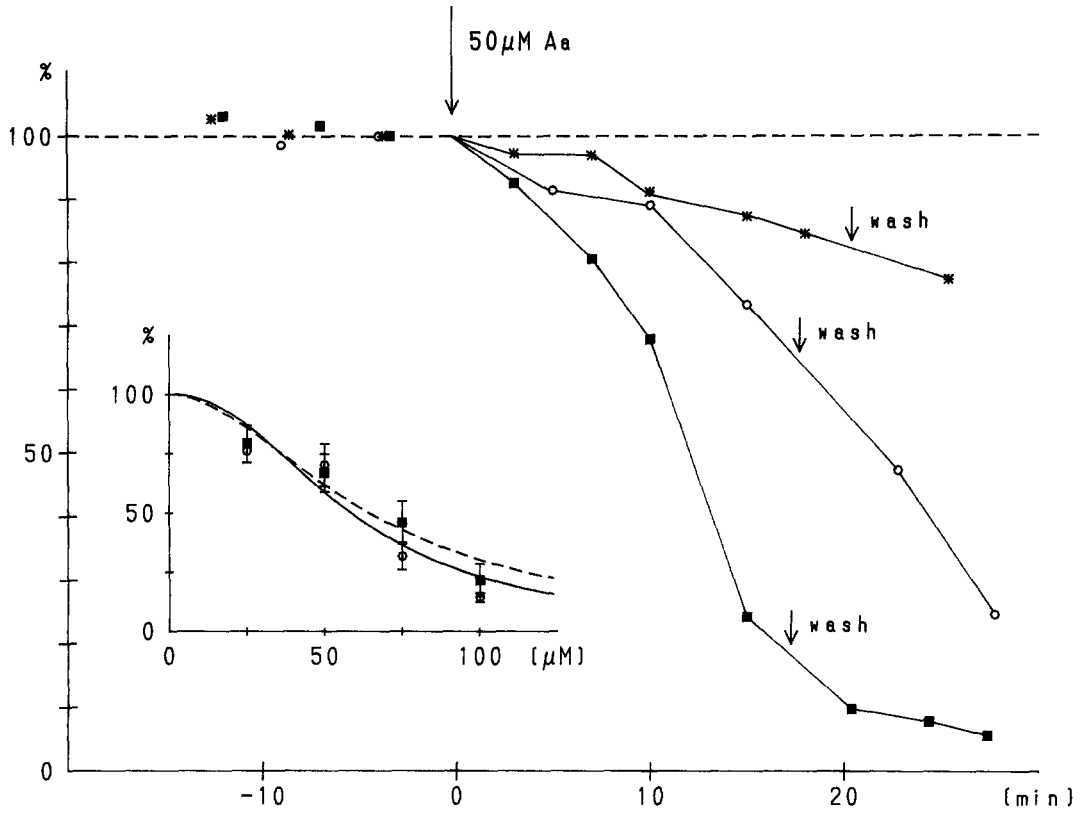

Fig. 3. The block of I_{Ca} by 50 μM AA develops slowly. I_{Ca}, measured at +20 mV in three different experiments (■, ○, *; cell capacitances 48, 69, 65 pF) plotted against time. I_{Ca} expressed in the percentage of last control measurement taken 3–4 min before application of AA. Wash with AA-free solution starts at ↓. Inset: Concentration-response curve for l-v-a (○) and h-v-a (■) Ca^{2+} current measured at −20 or −10 mV and at +20 mV, respectively. Application time 15 min. Averages ± SEM from 4–7 experiments. Points fitted with Eq. (2) with IC_{50} = 58.6 μM, n = 2.24 for ○ and IC_{50} = 64.5 μM, n = 1.90 for ■. Fit weighted according to the number of experiments.

and h-v-a I_{Ca} to 86.3 ± 3.6% of control (n = 12). The effect varied from cell to cell. Only in 7 out of 17 cells did 25 μM AA reduce l-v-a I_{Ca} to less than 85% of control. As mentioned above, the inhibition of I_{Ca} by 25 μM AA became more pronounced with increasing time. After 15 min, peak l-v-a and h-v-a I_{Ca} were reduced to 76.0 ± 5.0% (n = 7) and 79.0 ± 7.9% (n = 6), respectively.

Effect of 50–100 μM AA

The observation that AA reduces I_{Ca} continually with increasing time of application was supported by experiments with 50–100 μM AA. Figure 3 illustrates the progressive decrease of h-v-a I_{Ca}, measured at +20 mV, with increasing application time of 50 μM AA in three different cells. As in Fig. 2*B* the rate of current decline became approximately constant after the first 5 min. Between 10 and 15 min the rate was −0.8, −3.1 and −8.7% of control per min for the three cells of Fig. 3 and −4.5 and −3.6% per min in Fig. 2*B* at +30 and −20 mV, respectively. The rate of current decline varied greatly between cells and was similar for l-v-a and h-v-a I_{Ca}. The latter point was also tested in an experiment with 75 μM AA. We obtained −2.2 and −3.0% per min for l-v-a I_{Ca} (at −20 mV) and h-v-a I_{Ca} (at +20 mV), respectively, both measured between 10 and 15 min.

The inset of Fig. 3 shows the concentration-response curves for l-v-a I_{Ca} (○) and h-v-a I_{Ca} (■), based on currents measured after 15-min application of AA. The curves for the two types of current are very similar, the concentration for half inhibition (IC_{50}) being 59 and 65 μM, respectively.

Partial Reversibility of the AA Effect

Reversibility of the AA effect was poor (*see* Fig. 3). In some experiments partial recovery, at best 50%, could be achieved. In others no recovery at all occurred during a 10–20 min wash with AA-free bath solution. We tried to improve reversibility by washing with bovine serum albumin (BSA) (1–5 mg/ml), but found that BSA itself increases l-v-a I_{Ca} markedly, resulting in an apparent overrecovery from the fatty acid effect (*see* [31]).

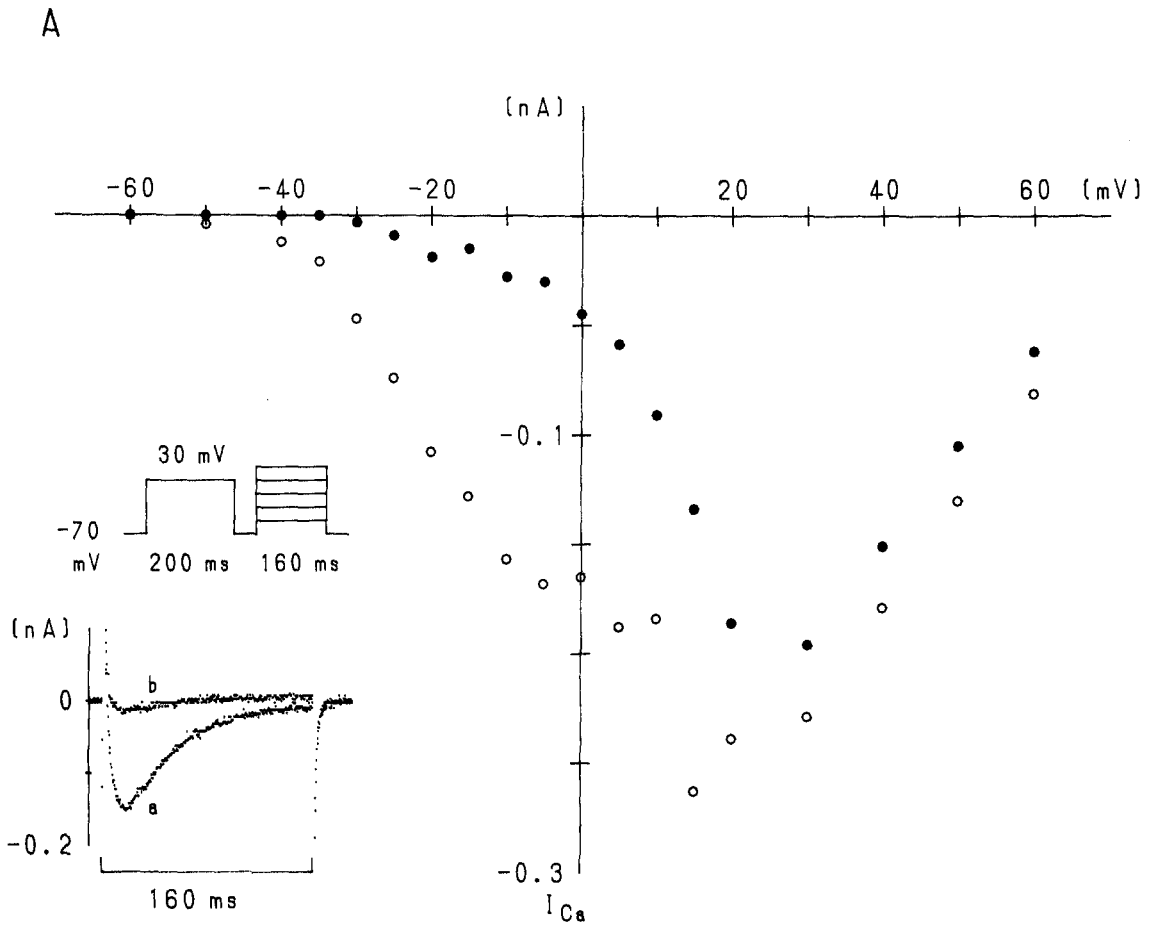
A
[nA]
-60
-40
-20
20
40
60 [mV]
-0.1
-0.3
I_{Ca}
30 mV
-70
mV
200 ms
160 ms
[nA]
0
-0.2
b
a
160 ms

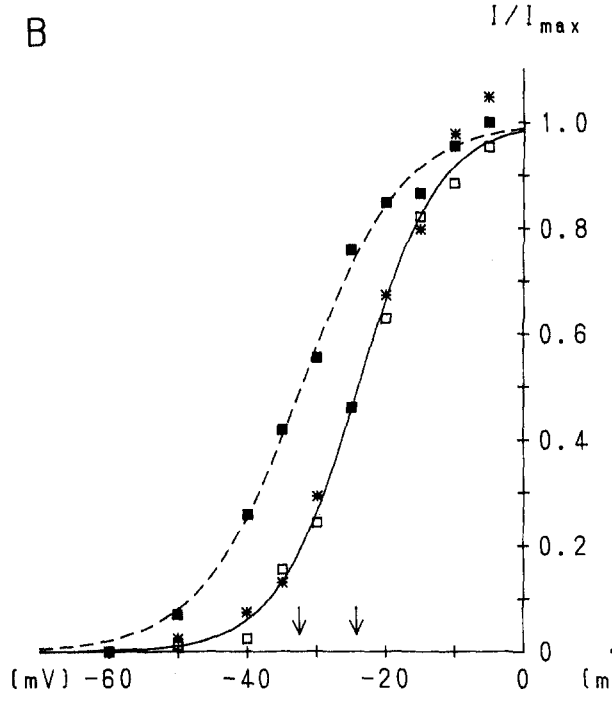
B
I/I_{max}
1.0
0.8
0.6
0.4
0.2
0
[mV] -60
-40
-20
0

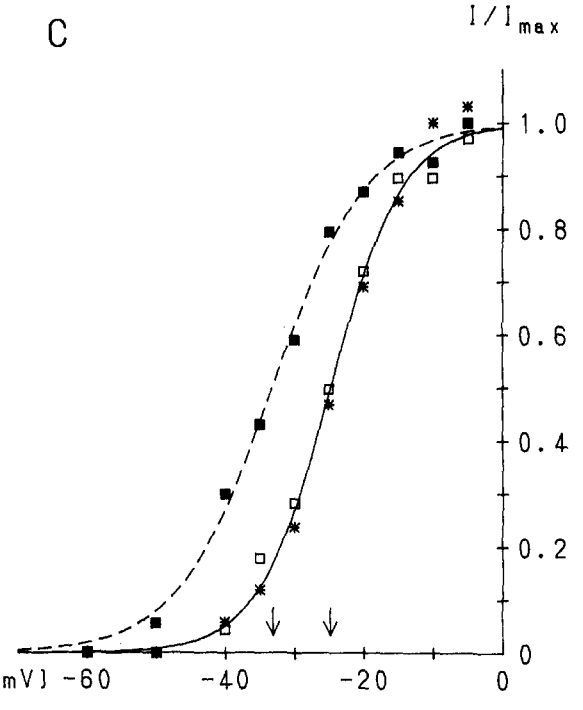
C
I/I_{max}
1.0
0.8
0.6
0.4
0.2
0
[mV] -60
-40
-20
0

AA Causes a Small Negative Shift of the Activation and Inactivation Curve of the l-v-a Ca^{2+} Current

As noted by [6], it is possible to inactivate the l-v-a Ca^{2+} current of NG108-15 cells selectively by using a 200 msec prepulse to about +30 mV followed by a 50 msec gap (*see* Fig. 5 of [6]). In Fig. 4 we used this pulse protocol (*see* inset) to determine the activation curve of the l-v-a I_{Ca}. *A* shows the current-voltage curves measured without (○) and with (●) prepulse. The difference between ○ and ● is the l-v-a I_{Ca}. It reaches a flat maximum at −5 mV. The difference, normalized to the maximum at −5 mV, has been plotted against pulse potential in *C* (*) together with points from a second series of measurements (□), yielding the activation curve of the l-v-a I_{Ca} (half potential V_o = −24.7 mV). A very similar curve (V_o = −24.0 mV) is obtained by taking simply the current without prepulse, measured at negative pulse potentials (○ in *A*), and plotting it, after normalization to I_{max} at −5 mV, against pulse potential (*B*).

The measurements were repeated in 25 μM AA, applied for 10–15 min. As shown by points ■ in Fig. 4*C*, the activation curve in 25 μM AA is slightly flatter than the control curve and its half potential V_o shifted by −8.3 mV. The maximum difference at −5 mV, taken as I_{max}, was 135 pA in control and 107 pA in 25 μM AA, a reduction to 79%. The curves in Fig. 4*B*, which were obtained directly from I_{Ca} without prepulse, indicate a very similar V_o shift of −8.5 mV and a decrease of I_{max} to 70%. In the experiment shown in Fig. 2, which was analyzed using the simpler method of Fig. 4*B*, V_o was −28.8 mV in control and −33.9 mV after 15 min in 25 μM AA and the slope factor k changed from −5.2 to −7.8 mV, respectively.

Likewise a small negative shift of the inactivation curve occurred. An experiment with 50 μM AA is illustrated in Fig. 5. The half potential V_o was stable at −34.4 mV in two control measurements and became −37.8, −39.2 and −40.6 mV after 3, 7 and 10 min in 50 μM AA (*see* inset of Fig. 5). In another experiment, V_o was −37.8 and −38.0 mV in the first and second control measurement and shifted to −45.4 mV after 3 min in 50 μM AA. A small effect on the inactivation curve was also seen with 25 μM AA. After 10 min in 25 μM AA, I_{max} was on average reduced to 81.2 ± 8.6% of control and V_o shifted by −4.4 ± 1.8 mV (n = 5).

The AA Effect is not Prevented by ETYA or PKC 19-31 Peptide and not Mimicked by Phorbol Ester

5, 8, 11, 14-eicosatetraynoic acid (ETYA), an inhibitor of lipoxygenase, cyclooxygenase and epoxygenase (for IC_{50} values, *see* [4, 28]), applied in the bath solution in a concentration of 25–50 μM for 7–21 min, had itself no effect on l-v-a and h-v-a I_{Ca} (n = 4). ETYA (50 μM) in the pipette solution did not prevent the reduction of I_{Ca} by 50 μM AA, suggesting that the latter is not mediated by an AA metabolite. In these experiments, AA was applied 16–21 min after break-through to whole-cell mode, giving the ETYA sufficient time to diffuse from the pipette into the cell. Without ETYA, 50 μM AA reduced I_{Ca} at −20 or −10 mV within 15 min to 70.1 ± 8.9% of control (n = 7), with ETYA to 70.7 ± 2.9% of control (n = 3). For I_{Ca} at +20 mV, the reduction was to 66.9 ± 7.9% of control (n = 7) without ETYA and to 78.3 ± 8.5% of control (n = 3) with ETYA.

In previous M current experiments [29], we observed a reduction of l-v-a I_{Ca} by 25 μM AA even when the pipette solution contained 1 μM PKC 19–31 peptide, a potent PKC inhibitor. In these experiments, l-v-a Ca^{2+} currents occurred when stepping from a strongly negative potential to −30 or −20 mV. Application of 25 μM AA for 10 min reduced them to 69.6 ± 8.7% of control (n = 8). With PKC 19–31 peptide, the reduction was smaller, namely to 84.5 ± 1.8% of control (n = 4), but the difference was not significant.

Phorbol 12, 13-dibutyrate (PDBu), an activator of PKC, did not affect the Ca^{2+} current of NG108-15 cells, confirming earlier work [3, 16] and making it further unlikely that the reduction of AA is mediated by PKC as found in hippocampal neurons [17]. Even at the high

Fig. 4. Separation of l-v-a and h-v-a Ca^{2+} current by the prepulse method [6]. (*A*) Current-voltage curve measured without (○) and with (●) prepulse. Inset shows pulse protocol (200 msec prepulse to 30 mV followed after 50 msec pause by 160 msec test pulses) and current samples (pulse potential −5 mV) without (a) and with (b) prepulse. (*B*) and (*C*) Estimates of the activation curve of the l-v-a Ca^{2+} current. (*B*) I_{Ca} without prepulse (normalized to its value at −5 mV) plotted against *V* for negative pulse potentials. (*C*) Difference (I_{Ca} without prepulse — I_{Ca} with prepulse) normalized and plotted against *V*. Symbols *, □ and ■ in *B* and *C* refer, respectively, to the measurements in *A*, to a second series of measurements (12 min after the first) and to a series of measurements in 25 μM AA, applied for 10–15 min. Cell capacitance 30 pF. The ratios I/I_{max} in *B* and *C* were fitted by Eq. (1) with the following parameters:

					V_o [mV]	k [mV]
B	*	and	□	control	−24.0	−5.8
		■		AA	−32.3	−7.3
C	*	and	□	control	−24.7	−5.2
		■		AA	−33.2	−6.8

Half potentials V_o indicated by arrows.

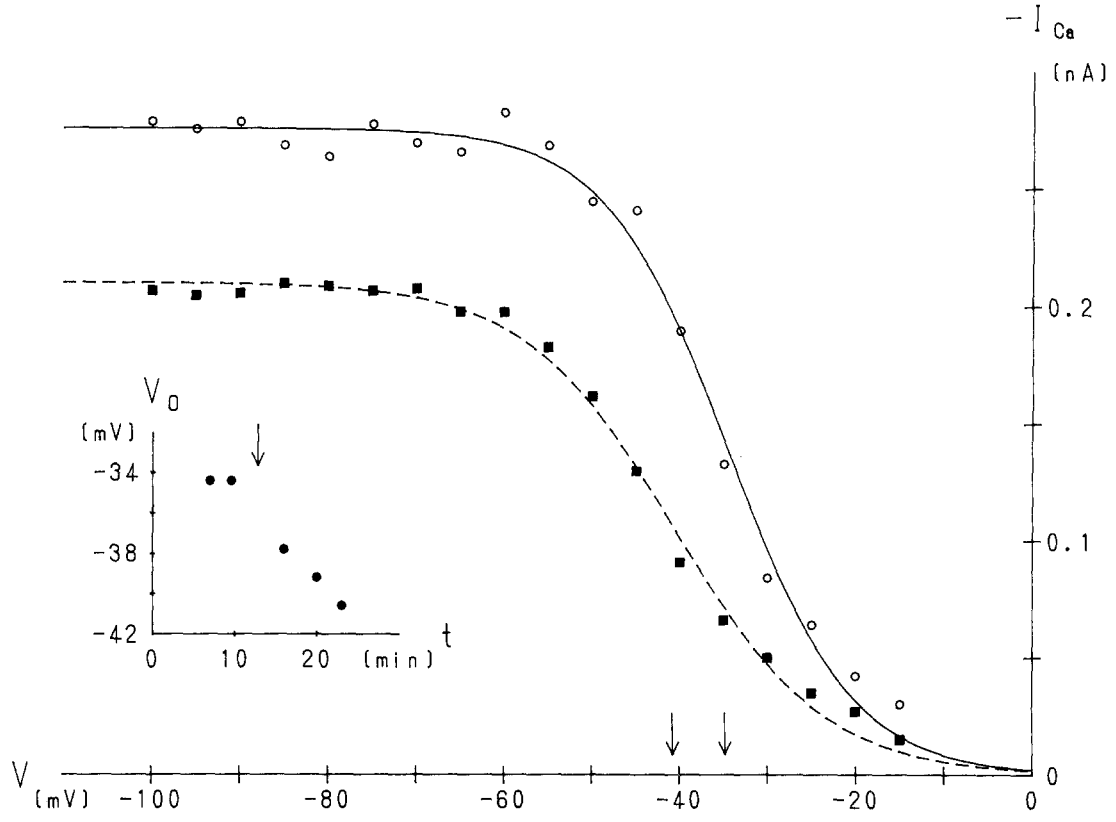

Fig. 5. Effect of 50 μM AA on the inactivation curve of the l-v-a Ca^{2+} current. ○, control; ■, 50 μM AA applied for 10 min. Points fitted with eqn (1) with the parameters $I_{max} = 0.28$ nA, $V_o = -34.4$ mV, $k = 7.0$ mV for ○ and $I_{max} = 0.21$ nA, $V_o = -40.6$ mV, $k = 8.5$ mV for ■. Half potentials V_o indicated by arrows. Inset: V_o plotted against time after break-through to whole-cell mode. Cell capacitance 53 pF.

concentration of 1 μM, PDBu did not reduce the peak or the sustained Ca^{2+} inward current. In our previous M current experiments [29], 0.1 μM PDBu partly inhibited the M current, but in the same cell failed to affect the l-v-a Ca^{2+} current.

Myristic Acid, Oleic Acid and Lysophosphatidate are Less Effective than AA

We also tested two other fatty acids, namely myristic and oleic acid, and the negatively charged palmitoyl lysophosphatidate (PLP). Myristic and oleic acid reduced l-v-a and h-v-a I_{Ca}, but were much less effective than AA. Myristic acid (50 μM) applied for 10 min decreased l-v-a I_{Ca} at −20 mV to 82% (n = 1) and h-v-a I_{Ca} at +20 mV to 77.0 ± 4.0% (n = 2). Following [7], who found octanoic acid more effective at lower pH, we tried to increase the effectiveness of myristic acid by lowering the pH of the bath to 6.5. However, the effect remained weak: decrease of l-v-a I_{Ca} to 86.5 ± 1.8% (n = 4) and of h-v-a I_{Ca} to 82.0 ± 5.0%. To demonstrate the weak effect of myristic acid convincingly we increased the concentration to 100 μM and applied the same pulse every 30 sec. As shown in Fig. 6, there was a small, reversible decrease of h-v-a I_{Ca} by myristic acid; a similar effect was demonstrated for l-v-a I_{Ca} with repetitive pulses (30 sec apart) to −30 mV.

The effect of 50 μM oleic acid was also weak and difficult to distinguish from a spontaneously occurring current change. A genuine small reduction of I_{Ca} measured at −10 mV or at +20 mV was seen in 2 or 3, respectively, out of 5 experiments. At −10 mV the decrease was to 83.5 ± 0.5% of control (n = 2) and at +20 mV to 88.0 ± 4.0% (n = 3), both for 10 min-application time. In NIE-115 neuroblastoma cells, 50 μM oleic acid inhibit peak and sustained I_{Ca} more strongly, namely by 27–44% [19]. We found that oleic acid like AA slightly increased I_{Ca} at −40 and −30 mV, the increase being superimposed on the usual slow spontaneous increase.

Palmitoyl lysophosphatidate (PLP) in a concentration of 25 μM had no reproducible effect on l-v-a and h-v-a I_{Ca}. At 50 μM it caused a reversible increase of the leakage current (n = 4), an effect never seen with AA. It also decreased I_{Ca}, but the increase in leakage made a quantitative estimate difficult.

Tetradecyltrimethylammonium (C_{14}TMA) and Sphingosine Act Differently from the Fatty Acids

The effect of the positively charged compounds tetradecyltrimethylammonium (C_{14}TMA) and sphingosine dif-

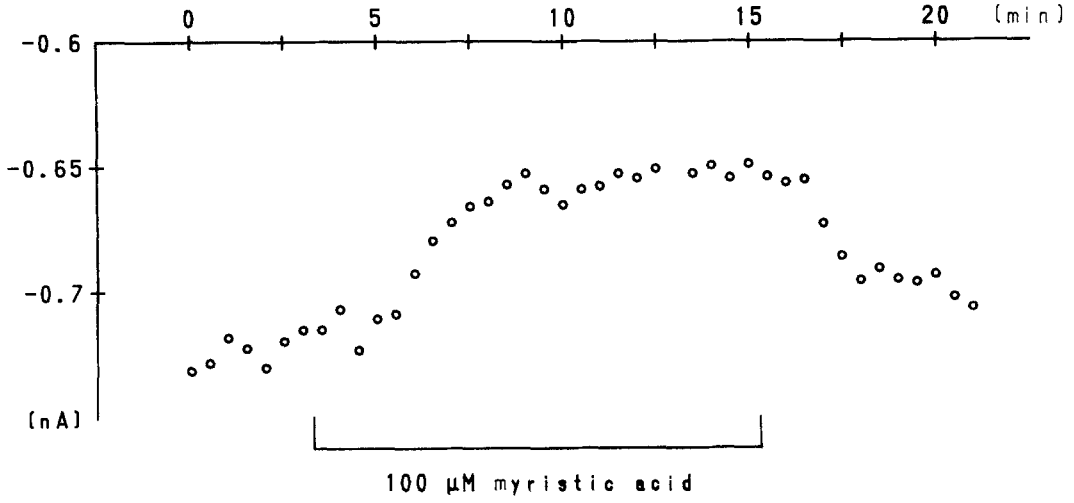

Fig. 6. Effect of 100 μM myristic acid on the h-v-a Ca^{2+} current. Pulse to +20 mV applied every 30 sec. Bath pH 6.5. Cell capacitance 100 pF.

fered in several respects from that of the fatty acids. C_{14}TMA, known as a cationic detergent and a blocker of Na^+ channels [8, 35] and K^+ channels [25], was surprisingly effective. As seen in Fig. 7, 5 μM C_{14}TMA strongly reduced the l-v-a I_{Ca} (and increased its time to peak, *see* original records in upper inset of Fig. 7) and moderately reduced the h-v-a I_{Ca}, the former effect being partly reversible. Closer inspection reveals two important details: (i) the points measured after 4–6 min in C_{14}TMA (●) coincide with those measured after 14–16 min (■), indicating that the C_{14}TMA effect has reached a steady-state at 4–6 min or earlier; (ii) the half potential for the activation of l-v-a I_{Ca}, V_o, shifts from –27 mV in control to –19 mV in 5 μM C_{14}TMA, as estimated from the Ca^{2+} currents at negative potentials, normalized to their value at –5 or 0 mV. This contrasts with the AA effect which does not reach a steady-state and shifts V_o to more negative potentials.

On average, 5 μM C_{14}TMA reduced l-v-a I_{Ca} to 23.3 ± 3.2% and h-v-a I_{Ca} to 79.3 ± 8.8% and shifted V_o by +9.0 ± 1.0 mV (n = 3). Raising the concentration to 10 or 50 μM caused a stronger reduction of the currents. It also increased the leakage (as expected for a detergent), but the increase was reversible. Lowering the concentration to 1 μM still produced a small current decrease. The concentration-response curve (*see* lower inset of Fig. 7) yielded an IC_{50} of 4.2 μM for the effect on l-v-a I_{Ca}. Repetitive pulsing (0.5–2 Hz) decreased l-v-a I_{Ca} in 1 μM C_{14}TMA further, but the decrease was hardly more pronounced than the attenuation during repetitive pulsing in control solution (*see* Fig. 7 of [34]).

Sphingosine, a sphingolipid metabolite which inhibits PKC and is thought to be a second messenger (for review, *see* [10, 20]), acted in all details similar to C_{14}TMA, but was less potent. At a concentration of 10 μM, sphingosine reduced l-v-a I_{Ca} to 51.0 ± 4.5% (n = 4) and h-v-a I_{Ca} slightly (but significantly) less, namely to 64.8 ± 2.5% (n = 4). It shifted V_o on average by +2.9 ± 1.2 mV (n = 4). At higher concentrations (25–50 μM) and sometimes at 10 μM, sphingosine increased the leakage current. Similar to the C_{14}TMA effect, that of sphingosine reached a steady-state within 5–10 min and could be partly reversed by 10–15 min washing. N-acetylsphingosine, a sphingosine analog without inhibitory action on PKC [11], applied in a concentration of 10 μM for 10 min, reduced l-v-a I_{Ca} to 89.3 ± 3.4% (n = 4) and h-v-a I_{Ca} to 80.0 ± 6.8% (n = 3), i.e., was less effective than sphingosine itself.

Discussion

Interpretation of the Experimental Findings

The main experimental findings are: (i) AA decreases l-v-a and h-v-a I_{Ca} about equally, an effect increasing with time without ever reaching a steady level of inhibition, probably reflecting continuous AA accumulation in the cell (*see* similar findings with octanoic acid on squid axons [7] and with the lipophilic drug U88779E on NIE-115 cells [13]); the decrease in current is difficult to reverse and is accompanied by a slight negative shift of the activation and inactivation curve of l-v-a I_{Ca}; the AA effect seems neither due to an AA metabolite nor to activation of PKC. (ii) Oleic and myristic acid also decrease l-v-a and h-v-a I_{Ca} but are much less potent than AA. (iii) Positively charged compounds like C_{14}TMA and sphingosine also reduce l-v-a and h-v-a I_{Ca} but act differently from AA; their effect reaches a steady-state within 5–10 min, is readily reversible and accompanied by a positive shift of the l-v-a I_{Ca} activation curve; the latter explains at least partly why the positively charged analogs decrease l-v-a I_{Ca} more than h-v-a I_{Ca}.

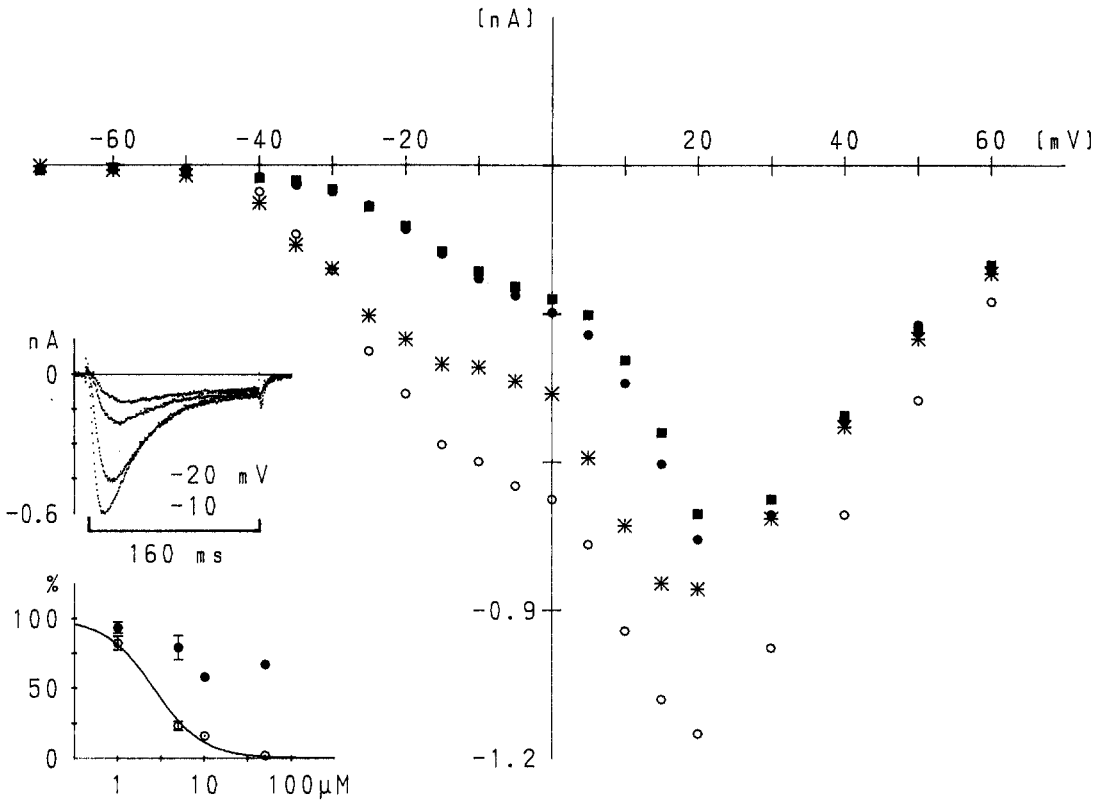

Fig. 7. Effect of 5 µM tetradecylammonium (C_{14}TMA) on l-v-a and h-v-a I_{Ca}. Current-voltage curve in control (○), in 5 µM C_{14}TMA for 4–6 min (●) and for 14–16 min (■) and after 12–14 min wash (*). Upper inset: Currents at −20 and −10 mV in control and in 5 µM C_{14}TMA for 14 min (small currents). Lower inset: Concentration-response curve for l-v-a (○) and h-v-a (●) I_{Ca} measured at −20 and +20 to +40 mV, respectively. Application time 5–8 min. Averages ± SEM from 6 and 3 experiments with 1 and 5 µM, respectively. One experiment each with 10 and 50 µM. Points fitted with an equation corresponding to Eq. (2) with IC_{50} = 4.2 µM and n = 1.52. Note logarithmic abscissa scale.

Our findings are consistent with the following ideas: (i) AA in its unionized form rapidly moves across the lipid bilayer [15] and, at the inner side of the membrane, reacts with the channel protein; likewise, AA blocks Cl^- channels only from the inner side of the membrane (*see* [36] and references therein). (ii) Oleic and myristic acid also move rapidly across the bilayer [15] but are less suited for interaction with proteins than AA with its particular structural and dynamic properties [27], hence much less effective. (iii) C_{14}TMA can incorporate its hydrophobic tail into the lipid bilayer but because of its permanent positive charge cannot permeate easily [8, 35]. Adsorption of C_{14}TMA cations to the outer edge of the membrane accounts for the positive shift of the l-v-a I_{Ca} activation curve; by analogy, the negative shift observed with AA may reflect adsorption of AA anions. (iv) C_{14}TMA not only blocks Na^+ and K^+ channels [8, 35, 25] but also Ca^{2+} channels; as suggested for Na^+ channels [35], the hydrophobic tail with its 14 methylene groups binds to a hydrophobic region of the channel pore and the hydrophilic head blocks the pore at its narrowest point. (v) The positively charged sphingosine acts in principle like C_{14}TMA but is a less potent Ca^{2+} channel blocker; addition of an acetyl group further reduces its potency.

Comparison with Previous Work

The first who compared the effect of a fatty acid with that of the corresponding alkyltrimethylammonium were Elliott, Haydon and Hendry [7], investigating octanoic acid (8:0) and C_8TMA on the squid axon. External or internal octanoic acid in a concentration as high as 5 mM at pH 7.4 produced only a small suppression of I_{Na}, whereas internal (but not external) application of 5 mM C_8TMA completely blocked peak I_{Na}. Similarly, we found a weak effect of myristic acid (14:0) and a surprisingly strong effect of C_{14}TMA on I_{Ca}. In [7] and in our work, the fatty acid and the alkyl-TMA acted both inhibitory. By contrast, [23–26] found K^+ channel activity increased by fatty acids and negatively charged lipids, but decreased by positively charged compounds (*see* Introduction). While in other preparations such as avian ciliary neurons [18] or guinea-pig hippocampus [17] the inhibition of Ca^{2+} current by 10–100 µM AA is mediated by

AA metabolites or PKC, our effect on I_{Ca} seems to be a direct effect of AA, resembling the inhibitory effect of AA (10–30 μM) on I_{Ca} of intestinal smooth muscle [32].

In some respects, the effect of AA on the Ca^{2+} current, I_{Ca}, of NG108-15 cells resembles its effect on the M current, I_M, of these cells while in other respects it is fundamentally different. Similar to the effect on I_{Ca}, the decrease of I_M is accompanied by a shift of the *M* conductance curve to more negative potentials [2]. Like the AA effect on I_{Ca}, the effect on I_M is highly variable from cell to cell [29] and difficult to reverse (*see* the very slow reversal of the 5 μM AA effect in Fig. 4 of [2]). However, unlike the AA effect on I_{Ca} the AA inhibition of I_M can be mimicked by PDBu and prevented by the PKC 19–31 peptide, i.e., is mediated by activation of PKC [29]. Also, inhibition of I_M by AA occurs fast, much faster than inhibition of I_{Ca}, and is observed with AA concentrations down to 3 or 5 μM [2, 29].

Whereas [25] observed an AA-like effect of palmitoyl lysophosphatidate (PLP) on K^+ channel activity in cell-attached and excised patches of smooth muscle, we did not find a reproducible effect of 25 μM PLP on Ca^{2+} currents of NG108-15 cells. According to [14], it is only in serum-starved NG108-15 cells that nanomolar lysophosphatidate concentrations evoke a transient rise in $[Ca^{2+}]_i$ and cell rounding.

Acknowledgment. We thank the Deutsche Forschungsgemeinschaft (SFB 246) for financial support, Dr. Timothy D. Plant (Homburg-Saar) for helpful discussions and Mrs. Heidi Löhr for technical assistance. We also thank Professor H.H. Wellhöner (Hannover) and Prof. G. Reiser (Magdeburg) for providing the NG108-15 cells.

References

1. Becchetti, A., Arcangeli, A., Del Bene, M.R., Olivotto, M., Wanke, E. 1992. Intra and extracellular surface charges near Ca^{2+} channels in neurons and neuroblastoma cells. *Biophys. J.* **63:**954–965
2. Béhé, P., Sandmeier, K., Meves, H. 1992. The effect of arachidonic acid on the M current of NG108-15 neuroblastoma x glioma hybrid cells. *Pfluegers Arch.* **422:**120–128
3. Brown, D.A., Docherty, R.J., McFadzean, I. 1989. Calcium channels in vertebrate neurons. Experiments on a neuroblastoma hybrid model. *Ann. N.Y. Acad. Sci.* **560:**358–372
4. Capdevila, J., Gil, L., Orellana, M., Marnett, L.J., Mason, J.I., Yadagiri, P., Falck, J.R. 1988. Inhibitors of cytochrome P-450 dependent arachidonic acid metabolism. *Arch. Biochem. Biophys.* **261:**257–263
5. Chizhmakov, I.V., Klee, M.R. 1994. The action of a phorbol ester on voltage-dependent parameters of the sodium current in isolated hippocampal neurons. *Neuroscience* **59:**285–290
6. Docherty, R.J. 1988. Gadolinium selectively blocks a component of calcium current in rodent neuroblastoma x glioma hybrid (NG108-15) cells. *J. Physiol.* **398:**33–47
7. Elliott, J.R., Haydon, D.A., Hendry, B.M. 1984. The asymmetrical effects of some ionized *n*-octyl derivatives on the sodium current of the giant axon of *Loligo forbesi*. *J. Physiol.* **350:**429–445
8. Elliott, J.R., Haydon, D.A., Hendry, B.M. 1985. Dual effects of internal *n*-alkyltrimethylammonium ions on the sodium current of the squid giant axon. *J. Physiol.* **361:**47–64
9. Fernandez, J.M., Fox, A.P., Krasne, S. 1984. Membrane patches and whole-cell membranes: a comparison of electrical properties in rat clonal pituitary (GH_3) cells. *J. Physiol.* **356:**565–585
10. Hannun, Y.A., Bell, R.M. 1989. Functions of sphingolipids and sphingolipid breakdown products in cellular regulation. *Science* **243:**500–507
11. Hannun, Y.A., Loomis, C.R., Merrill, A.H. Jr., Bell, R.M. 1986. Sphingosin inhibition of protein kinase C activity and of phorbol dibutyrate binding *in vitro* and in human platelets. *J. Biol. Chem.* **261:**12604–12609
12. Herman, M.D., Reuveny, E., Narahashi, T. 1993. The effect of polyamines on voltage-activated calcium channels in mouse neuroblastoma cells. *J. Physiol.* **462:**645–660
13. Im, H.K., Im, W.B., Tsuzuki, K. 1993 Selective block of transient Ca channel current in mouse neuroblastoma cells by U-88779E. *J. Pharmacol. Exp. Ther.* **265:**529–535
14. Jalink, K., Eichholtz, T., Postma, F.R., van Corven E.J., Moolenaar, W.H. 1993. Lysophosphatidic acid induces neuronal shape changes via a novel, receptor-mediated signaling pathway: similarity to thrombin action. *Cell Growth Diff.* **4:**247–255
15. Kamp, F., Hamilton, J.A. 1993. Movement of fatty acids, fatty acid analogues, and bile acids across phospholipid bilayers. *Biochemistry* **32:**11074–11086
16. Kasai, H. 1992. Voltage- and time-dependent inhibition of neuronal calcium channels by a GTP-binding protein in a mammalian cell line. *J Physiol.* **448:**189–209
17. Keyser, D.O., Alger, B.E. 1990. Arachidonic acid modulates hippocampal calcium current via protein kinase C and oxygen radicals. *Neuron* **5:**545–553
18. Khurana, G., Bennett, M.R. 1993. Nitric oxide and arachidonic acid modulation of calcium currents in postganglionic neurones of avian cultured ciliary ganglia. *Br. J. Pharmacol.* **109:**480–485
19. Linden, D.J., Routtenberg, A. 1989. *Cis*-fatty acids, which activate protein kinase C, attenuate Na^+ and Ca^{2+} currents in mouse neuroblastoma cells. *J. Physiol.* **419:**95–119
20. Merrill, A.H. Jr., Steven, V.L. 1989. Modulation of protein kinase C and diverse cell functions by sphingosine — a pharmacologically interesting compound linking sphingolipids and signal transduction. *Biochim. Biophys. Acta* **1010:**131–139
21. Meves, H. 1994. Modulation of ion channels by arachidonic acid. *Prog. Neurobiol.* **43:**175–186
22. Miller, B., Sarantis, M., Traynelis, S.F., Attwell, D. 1992. Potentiation of NMDA receptor currents by arachidonic acid. *Nature* **355:**722–725
23. Ordway, R.W., Singer, J.J., Walsh, J.V. 1991. Direct regulation of ion channels by fatty acids. *Trends Neurosci.* **14:**96–100
24. Ordway, R.W., Wals J.V., Singer, J.J. 1989. Arachidonic acid and other fatty acids directly activate potassium channels in smooth muscle cells. *Science* **244:**1176–1179
25. Petrou, S., Ordway, R.W., Hamilton, J.A., Walsh, J.V., Singer, J.J. 1994. Structural requirements for charged lipid molecules to directly increase or suppress K^+ channel activity in smooth muscle cells. Effects of fatty acids, lysophosphatidate, acyl coenzyme A and sphingosine. *J. Gen. Physiol.* **103:**471–486
26. Petrou, S., Ordway, R.W., Singer, J.J., Walsh, J.V. 1993. A putative fatty acid-binding domain of the NMDA receptor. *Trends in Biochem. Sci.* **18:**41–42
27. Rich, M.R. 1993. Conformational analysis of arachidonic and related fatty acids using molecular dynamics simulations. *Biochim. Biophys. Acta* **1178:**87–96
28. Salari, H., Braquet, P., Borgeat, P. 1984. Comparative effects of indomethacin, acetylenic acids, 15-HETE, nordihydroguaiaretic

acid and BW755C on the metabolism of arachidonic acid in human leukocytes and platelets. *Prostaglandins, Leukotrienes and Medicine* **13:**53–60

29. Schmitt, H., Meves, H. 1993. Protein kinase C as mediator of arachidonic acid-induced decrease of neuronal M current. *Pfluegers Arch.* **425:**134–139
30. Schmitt, H., Meves, H. 1994. Arachidonic acid inhibits neuronal calcium current and shifts its voltage dependence. *Pfluegers Arch.* **426:**Suppl:R59
31. Schmitt, H., Meves, H. 1994. Bovine serum albumin selectively increases the low-voltage-activated calcium current of NG108-15 neuroblastoma x glioma cells. *Brain Res.* **656:**375–380
32. Shimada, T., Somlyo, A.P. 1992. Modulation of voltage-dependent Ca channel current by arachidonic acid and other long-chain fatty acids in rabbit intestinal smooth muscle. *J. Gen. Physiol.* **100:**27–44
33. Tsunoo, A., Yoshii, M., Narahashi, T. 1986. Block of calcium channels by enkephalin and somatostatin in neuroblastoma-glioma hybrid NG108-15 cells. *Proc. Natl. Acad. Sci. USA* **83:**9832–9836
34. Twombly, D.A., Yoshii, M., Narahashi, T. 1988. Mechanisms of calcium channel block by phenytoin. *J. Pharmacol. Exp. Therap.* **246:**189–195
35. Wang, G.K., Simon, R., Wang, S.-Y. 1991. Quaternary ammonium compounds as structural probes of single batrachotoxin-activated Na^+ channels. *J. Gen. Physiol.* **98:**1005–1024
36. Zachar, J., Hurnák, O. 1994. Arachidonic acid blocks large-conductance chloride channels in L6 myoblasts. *Gen. Physiol. Biophys.* **13:**193–213